



## Adsorption of bendamustine anti-cancer drug on Al/B-N/P nanocages: A comparative DFT study

NOSRAT MADADI MAHANI\*, REZA BEHJATMANESH-ARDEKANI  
and ROYA YOSEFELAHI

*Department of Chemistry, Payame Noor University (PNU), 19395-4697, Tehran, Iran*

(Received 12 March, revised 25 May, accepted 26 May 2022)

**Abstract:** Anti-cancer drug delivery based on nanocages is important step in drug development process due to reducing side effects and drug-releasing near the tumor cell. We have studied the interaction of the bendamustine anti-cancer drug with the Al/B-N/P nanocages with utilization density functional theory (DFT) approach both in gas and water phases at the B3LYP/6-31G (d,p) level of theory. Results show that the nanocages quantum parameters were somewhat varied by the adsorption of the bendamustine drug. The bendamustine drug operates as an electrons donor and can adsorb in the site of the electron's acceptor of nanocages. The changes in Gibbs energy correspond to a chemisorption in both phases. The results indicated that the bond between studied nanocages and bendamustine is covalent. However, all studied nanocages may be favorable candidates for detecting the bendamustine drug. Yet, pristine  $B_{12}P_{12}$  and  $B_{12}N_{12}$  nanocages appeared to be more suitable for drug delivery than  $Al_{12}P_{12}$  and  $Al_{12}N_{12}$  based on their recovery times.

**Keywords:** drug delivery; recovery time; interaction; covalent; molecular electrostatic potential (*MEP*); Gibbs energy; nanostructure.

### INTRODUCTION

Bendamustine belongs to alkylating agents<sup>1</sup> that can be used to treat various human cancers such as non-Hodgkin's lymphoma, multiple myeloma, chronic lymphocytic leukemia, lung cancer and sarcoma.<sup>2</sup>

Bendamustine contains a benzimidazole ring, a butyric acid side chain and a 2-chloroethylamine alkylating group (Fig. 1). Bendamustine is a chemotherapeutic drug with a different cytotoxicity type contrasted with typical alkylating agents. It has both alkylating and antimetabolite properties.<sup>3</sup> Nanocarriers could decrease toxic effects of drugs, especially anti-cancer drugs. In the past few years, the applications of boron nitride (BN) and aluminum nitride (AlN) nano-

\* Corresponding author. E-mail: nmmadady@gmail.com  
<https://doi.org/10.2298/JSC220312046M>

cages as drug delivery have increased due to their features such as high thermal stability, great adsorbing capacity and low toxicity.

Units of the boron nitride (BN) and aluminum nitride (AlN) create main groups of nanostructures, they are made in the combinations of nanosheets, nano-clusters, nano chains and nanocages.<sup>4</sup> Recently, it has been demonstrated that boron nitride (BN) and aluminum nitride (AlN) nanocages are nontoxic<sup>5</sup> and can be beneficial for pharmaceutical applications.

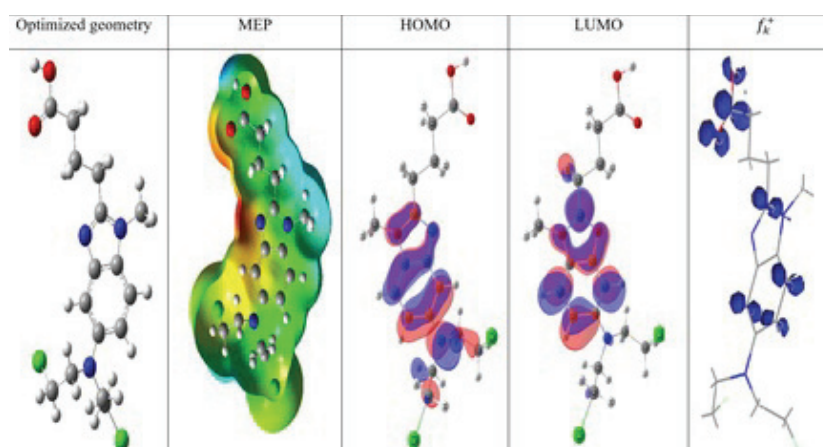


Fig. 1. Geometry optimization, molecular electrostatic potential (MEP),  $F^+$  descriptor and HOMO–LUMO depictions of bendamustine drug (solvent).

Due to their excellent properties, boron nitride nanotubes have been used as a new carrier for the purposed magnetic carrier of the drugs.<sup>6</sup> The previous studies have illustrated that B atoms are more reactive than nitrogen atoms for N containing functional groups for BN systems.<sup>7,8</sup> Also, it was reported that lithium-doped fullerenes are more reactive than the pristine fullerenes in reactions of 1,3 dipolar cycloaddition.<sup>9</sup> Soltani *et al.*<sup>10</sup> have investigated the optical and electronic features of 5-AVA-functionalized BN nanoclusters by DFT calculations. Also, 5-ALA functioned with B16N16 and B12N12 nanoclusters have been studied to investigate the electronic and structural properties. DFT studies have been performed for investigation interaction of melphalan anticancer drug and 24 atoms nanoclusters.<sup>11</sup>

The adsorption of histidine and tyrosine amino acids on Al<sub>12</sub>N<sub>12</sub> and B<sub>12</sub>N<sub>12</sub> nanocages has been studied to develop biochemical sensors for these amino acids.<sup>12</sup> The interaction between adipic acid and Al/B-N/P nanocages was investigated by DFT approach.<sup>13</sup> Soliman *et al.*<sup>14</sup> have studied adsorption of favipiravir drugs on fullerene and boron nitride nanocages by theoretical methods. Density functional theory studies have been carried out for the AlN nanotube, nanosheet and nanocage with benzoyl ethanamine drug.<sup>15</sup> Interaction between the jug-

lone and its derivative as antioxidant agents with  $B_{12}N_{12}$  nanocage have been investigated by density functional theory.<sup>16</sup> Also, DFT calculations have been performed for adsorption of guanine as a nucleobase on the surface of  $Al_{12}N_{12}$ ,  $Al_{12}P_{12}$ ,  $B_{12}N_{12}$  and  $B_{12}P_{12}$  nanocages.<sup>17</sup>

In the present study, we investigated and compared the interaction of bendamustine theoretically functionalized at  $B_{12}N_{12}$ ,  $B_{12}P_{12}$ ,  $Al_{12}N_{12}$  and  $Al_{12}P_{12}$  nanocages for the amelioration and design of nanocages ability for drug delivery. For investigation of the interaction between these nanocages with bendamustine drug, we studied quantum and thermodynamic descriptors. Free energies of binding, HOMO–LUMO frontier orbital diagrams, molecular electrostatic potential (*MEP*), density of state (DOS) plots, AIM and NBO analysis and time recovery for bendamustine drug desorption from studied nanocages.

## EXPERIMENTAL

The initial structure of  $B_{12}N_{12}$ ,  $B_{12}P_{12}$ , and  $Al_{12}N_{12}$ ,  $Al_{12}P_{12}$  and bendamustine drug were created using Gauss View 5.0 and optimized by density functional theory at the B3LYP/6-31g (d,p) level<sup>18</sup> of theory using the Gaussian 09 code<sup>19</sup> in the gas and the solvent phases. The formation a homogenous system, is one of the important parameters to achieve desired concentration of drug in systemic circulation for desired (anticipated) pharmacological response. As solvent (water) plays a major role in our body, it has been selected as a solvent in order to identify the interaction of bendumustine molecule with nanocages while passing through human bodies.

Thereinafter, complexes of bendamustine and nanocages were geometrically optimized. The B3LYP functional was an efficacious and accurate functional in nanostructure systems.<sup>20</sup> Frequency calculations were performed and demonstrated that there is no negative frequency in typical analyses. One of the aims of this research is foretelling the sensibility gap of the nanocages to the vicinity of bendamustine drug using the highest occupied (HOMO) and the lowest unoccupied molecular orbital (LUMO). The  $E_g$  is dependent on the conduction electron population ( $N$ ) and can be applied as benchmarks for an adsorbing sensibility that can be used as a suitable criterion for their adsorption:<sup>21</sup>

$$N = AT^{3/2} \exp(-E_g / 2kT) \quad (1)$$

where  $k$  is the Boltzmann constant and  $A$  (electrons  $m^3 K^{3/2}$ ) is a constant.

For the interaction of nanocages with bendamustine drug, the most stable complex nanocage–bendamustine was optimized on the gas phase and the water solvent employing the B3LYP/6-31G (d,p) level theory. The change in adsorption energy of bendamustine drug on nanocages has been obtained using the following equation:

$$\Delta G_{ad} = G_{\text{nanocage/bendamustine}} - (G_{\text{bendamustine}} + G_{\text{nanocage}}) \quad (2)$$

where  $G_{\text{nanocage/bendamustine}}$  is the Gibbs energy of the complex, *i.e.*, the interaction between anti-cancer bendamustine drug ( $G_{\text{bendamustine}}$ ) and the studied nanocages ( $G_{\text{nanocage}}$ ).

To investigate the electronic structure and the nature of the interaction of complexes, molecular electrostatic potential (MEP), HOMO–LUMO frontier orbital diagrams and density of states (DOS) were presented. This approach has been proven to be beneficial in the previous literature.<sup>22,23</sup> Furthermore, the calculation of quantum theory of atoms in molecules (QTAIM)<sup>24</sup> was performed for detailed investigation on bonding characteristics and to probe

the electron density of complexes. Atom in molecule (AIM) analysis was used to calculate intramolecular force. The electron density ( $\rho$ ), Laplacian of electron densities ( $\nabla^2\rho$ ) and ellipticity parameters ( $\varepsilon$ ) at the bond critical points for nanocages–bendamustine were calculated from AIM calculations *via* the AIM studio program.

## RESULTS AND DISCUSSION

The pristine nanocages consist of 6 tetragonal and 8 hexagonal rings that are not flattish.<sup>25</sup> Table I and Fig. 2 show the mean bond angles and bond lengths for Al–N, Al–P, B–N and B–P in tetragonal and hexagonal rings before and after adsorption. The mean bond lengths in the nanocages are longer in the  $\text{Al}_{12}\text{P}_{12}$  in both the hexagonal and the tetragonal rings. Although, the bond lengths of the hexagonal ring in nanocages are shorter than the tetragonal rings due to the more tension in the tetragonal rings compared to the hexagonal ones.

TABLE I. Selected bond lengths ( $D_1$  and  $D_2$ ) and bond angles  $A_1, A_2, A_3$  and  $A_4$  for nanocages (PCM)

Property	Ring	$\text{B}_{12}\text{N}_{12}$	$\text{B}_{12}\text{P}_{12}$	$\text{Al}_{12}\text{N}_{12}$	$\text{Al}_{12}\text{P}_{12}$
$D_1$ / nm	6	0.1440	0.1910	0.1798	0.2343
$D_2$ / nm	4	0.1486	0.1929	0.1861	0.2343
$A_1$ / ° (Al–N(P)–Al/B–N(P)–B)	6	111.0402	101.9178	112.7974	101.9178
$A_2$ / ° (N(P)–Al–N(P)/N(P)–B–N(P))	6	125.7739	129.5436	125.5935	129.9199
$A_3$ / ° (N(P)–Al–N(P)/N(P)–B–N(P))	4	98.2291	98.8408	94.5483	99.0950
$A_4$ / ° (Al–N(P)–Al/B–N(P)–B)	4	80.5001	76.1199	84.5106	74.8137

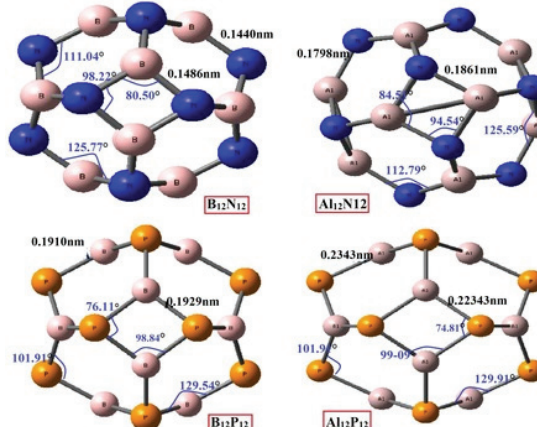


Fig. 2. Bond lengths and bond angles for nanocages (PCM).

The bond angles for N–Al–N in  $\text{Al}_{12}\text{N}_{12}$  nanocage are  $A_2 = 125.59^\circ$ ,  $A_3 = 94.54^\circ$ . Also, the bond angles for Al–N–Al are,  $A_1 = 112.79^\circ$  and  $A_4 = 84.51^\circ$ , in the hexagonal and tetragonal rings, respectively. Whereas, in the  $\text{B}_{12}\text{N}_{12}$  nanocage, the N–B–N angle has the values of  $A_2 = 125.77^\circ$ ,  $A_3 = 98.22^\circ$  and the B–N–B angle has the values of  $A_1 = 111.04^\circ$ , and  $A_4 = 80.46^\circ$ , in the hexagonal ring and

the tetragonal rings, respectively which are almost the same in both  $\text{Al}_{12}\text{N}_{12}$  and  $\text{B}_{12}\text{N}_{12}$  nanocages. The P–Al–P angle has the values of  $A_2 = 129.91^\circ$  and  $A_3 = 99.09^\circ$  and the Al–P–Al angle has the values of  $A_1 = 99.80^\circ$  and  $A_4 = 74.81^\circ$ , in the hexagonal ring and the tetragonal rings, respectively. While the P–B–P angle has the values of  $A_2 = 129.54^\circ$ ,  $A_3 = 98.84^\circ$  and the B–P–B angle has the values of  $A_1 = 101.91^\circ$  and  $A_4 = 76.11^\circ$  in the hexagonal ring and the tetragonal rings, respectively.

The lowest unoccupied molecular orbitals (LUMOs) and the highest occupied molecular orbitals (HOMOs) as the frontier molecular orbitals (FMOs) are the central orbitals that participate in chemical reactions. The HOMO signifies LUMO's capacity to supply an electron as an electron receptor.<sup>26</sup>

The difference between LUMO and HOMO, which is called the energy gap, displays structure stability.<sup>27</sup> Fig. 2 displays pictures of the HOMOs and LUMOs orbitals. The energy gap of the anti-cancer drug is observed to be 4.74 eV, which is reasonable for the pharmaceutical activity of the bendamustine drug.<sup>28–30</sup> Higher energy gap indicates less polarity of anticancer drug, which is recognized as a hard drug. Also, it indicates low chemical reactivity and suitable stability.

The strength of the vicinal charges, electrons and nuclei at a unique position was investigated by molecular electrostatic potential (*MEP*) in terms of colors.<sup>31,32</sup> *MEP* of the bendamustine drug in the PCM is illustrated in Fig. 2. The negative and positive positions are of the bendamustine drug are between  $-7.930 \times 10^{-2}$  and  $7.93 \times 10^{-2}$ .

The most positive region, as the nucleophilic site, is demonstrated by blue color and the most negative region, as the electrophilic site, is displayed by red color. The bendamustine drug, near the nitrogen atom N39, is more the negative and demonstrated by the red color. Around COOH functional group are also somewhat negative. The other segments of the drug are illustrated in the nucleophilic region. Therefore, the reactive regions of the drug represent biological activity.

To recognize reactivity sites for bendamustine drug, Fukui functions for electrophilic and nucleophilic attacks ( $f_k^+$ ,  $f_k^-$ ) has been studied<sup>33</sup> based on Mulliken population analysis, which has been calculated as:

$$f_k^+ = (q(N+1) - q(N)) \text{ for nucleophilic attack} \quad (3)$$

$$f_k^- = (q(N) - q(N-1)) \text{ for electrophilic attack} \quad (4)$$

Also, dual descriptor  $\Delta f(k)$  is obtained by following the formula:<sup>34</sup>

$$\Delta f(k) = f_k^+ - f_k^- \quad (5)$$

For the electrophilic attack,  $\Delta f(k)$  is negative, and for the nucleophilic attack,  $\Delta f(k)$  is positive.

Fukui indices for nucleophilic attack (Fukui (+))  $N$  (39) is equal 0.085, and for electrophilic attack (Fukui (-)) is equal 0.006. The trend of the dual Fukui

indices for nucleophilic attack is as follows N8 > N16 > N17. The negative dual descriptor for electrophilic attack is O21 > O22.

This study's primary purpose is to investigate the sensitivity of electronic properties of the Al<sub>12</sub>N<sub>12</sub>, Al<sub>12</sub>P<sub>12</sub>, B<sub>12</sub>N<sub>12</sub> and B<sub>12</sub>P<sub>12</sub> nanocages to the bendamustine drug. The results in Table II display that in all bendamustine/nanocage systems, the HOMO is unfixed, and the LUMO is fixed after the adsorption process of bendamustine drug; so, the  $E_g$  in them is reduced.

TABLE II. Chemical descriptors  $\sigma$  in both the gas and the solvent phases

Compound	Phase	$E_{\text{HOMO}}$ / eV	$E_{\text{LUMO}}$ / eV	$E_g$ / eV	$\eta$ / eV	$S$ / eV <sup>-1</sup>	$\chi$ / eV
B <sub>12</sub> N <sub>12</sub>	GAS	-7.7098	-0.8617	6.8480	3.4240	0.2920	4.2858
	PCM	-7.6997	-0.8002	6.8995	3.4497	0.2898	4.2500
B <sub>12</sub> P <sub>12</sub>	GAS	-6.8301	-3.1315	3.6986	1.8493	0.5407	4.9808
	PCM	-6.6347	-2.9051	3.7296	1.8648	0.5362	4.7699
Al <sub>12</sub> N <sub>12</sub>	GAS	-6.4717	-2.5393	3.9323	1.9661	0.5086	4.5055
	PCM	-6.5177	-2.4607	4.0569	2.0284	0.4929	4.4892
Al <sub>12</sub> P <sub>12</sub>	GAS	-6.7462	-3.3633	3.3829	1.6914	0.5912	5.0548
	PCM	-6.4488	-2.9045	3.5443	1.7721	0.5642	4.6767
Drug	GAS	-5.1255	-0.3757	4.7497	2.3748	0.4210	2.7506
	PCM	-5.1522	-0.4473	4.7048	2.3524	0.4250	2.7998
Al <sub>12</sub> P <sub>12</sub> -B	GAS	-5.5756	-2.4199	3.1557	1.5778	0.6337	3.9977
	PCM	-5.4921	-2.5091	2.9829	1.4914	0.6704	4.0006
B <sub>12</sub> N <sub>12</sub> -B	GAS	-5.7721	-1.4359	4.3361	2.1680	0.4612	3.6040
	PCM	-5.5198	-1.1243	4.3954	2.1977	0.4550	3.3221
B <sub>12</sub> P <sub>12</sub> -B	GAS	-5.5805	-2.3646	3.2158	1.6079	0.6219	3.9726
	PCM	-5.5440	-2.5905	2.9535	1.4767	0.6771	4.0673
Al <sub>12</sub> N <sub>12</sub> -B	GAS	-5.5560	-1.7227	3.8332	1.9166	0.5217	3.6394
	PCM	-5.4444	-1.8525	3.5919	1.7959	0.5568	3.6485

The drug losses more electrons basis on NBO charge analysis in the liquid phase to the nanocages than in the gas phase. For instance, a charge of 0.45 e is conducted from the drug to the AlN nanocage complex, but that is 0.25 e in the gas phase. Finally, the charge transfer in the liquid phase is more prominent than in the gas phase, as shown in Table III. Accordingly, it can be deduced that nanocages can diagnose bendamustine most positive region as the nucleophilic site drug according to Eq. (2). Since the electrical conductivity of the nanocages increased by decreasing the  $E_g$ , which can be transformed into an electrical signal that supports the detection process.

According to Zhan *et al.*<sup>35</sup> gap energy equals to,  $E_g = E_{\text{LUMO}} - E_{\text{HOMO}}$  chemical hardness equals to  $\eta = E_g/2$ , mulliken electronegativity equals to  $\chi = E_{\text{LUMO}} + E_{\text{HOMO}}$ , and the chemical softness equals to  $S = 1/\eta$  which is the opposite of hardness. The energy gap varies in the order BN > AlN > BP > AlP in pristine nanocages, also after complexation show the same trend.

TABLE III. Values of Gibbs energy change, recovery time, dipole moments and  $\Delta N$  for systems under study

Compound	Medium	$\Delta G / \text{kJ mol}^{-1}$	$\tau / \text{s}$	Dipole moment, D*	$\Delta N$
$\text{B}_{12}\text{N}_{12}-\text{B}$	Gas	-70.50	2.14	9.85	-0.38
	PCM	-83.05	$3.41 \times 10^2$	14.38	-0.41
$\text{B}_{12}\text{P}_{12}-\text{B}$	Gas	-45.77	$10^4$	11.49	-0.39
	PCM	-48.78	$3.00 \times 10^4$	15.95	-0.42
$\text{Al}_{12}\text{N}_{12}-\text{B}$	Gas	-117.57	$3.73 \times 10^8$	10.21	-0.27
	PCM	-126.18	$1.20 \times 10^{10}$	20.69	-0.45
$\text{Al}_{12}\text{P}_{12}-\text{B}$	Gas	-98.95	$2.05 \times 10^5$	16.14	-0.28
	PCM	-109.53	$1.46 \times 10^7$	23.68	-0.33

The  $E_g$  is decreased in all nanocages complexes compared to the pristine nanocages. Consequently, it is possible that the bendamustine drug can be sensed by nanocages based on the Eq. (1). Because the electrical conductivity of the nanocages will rise by reducing the  $E_g$  and help the detection process.

HOMO and LUMO of nanocages are on N and P, and considerable variations are observed for HOMO and LUMO on complexation with bendamustine drug, which is like the adsorption of guanine on these nanocages.<sup>36</sup>

The hardness values of AlN/AlP/BN/BP–bendamustine complexes are 1.79, 1.49, 2.19 and 1.47 eV, respectively. This shows, for all systems, the softness will increase after adsorption, but the hardness is decreased after adsorption.

In bendamustine nanocage systems, HOMO of AlN– AlP– and BP–bendamustine is located on the drug except for COOH group, and LUMO is situated on ALN nanocage.

Nevertheless, in BN–bendamustine, both HOMO and LUMO are spread over drugs except the COOH group. The distributions of HOMO and LUMO can change the band gap. Change in band gap upon complexation is 2.5 eV in BN, but changes in band gap are smaller in another nanocage. Therefore, the nanocages can be used as useful sensors for bendamustine because their electronic properties mainly change. Also, to determine the chemical activity of complexes, the MEPs surface of bendamustine with nanocages are investigated. Fig. 3 displays that N and P are negatively charged, while B and Al are positively charged.

The nanocages, due to the charge density, can act as the nucleophilic site. Dipole moments of pristine nanocages are zero. Significant changes are displayed in dipole moment after adsorption (Table III).

Dipole moments of AlN–bendamustine, AlP–bendamustine, BN–bendamustine, and BP–bendamustine are 20.69, 23.68, 14.37 and 15.94 D, respectively, in the solvent phase. The most increase is seen for AlP–bendamustine, followed by AlN–bendamustine nanocage. As well as BN–bendamustine complex has a low

\* 1 D =  $3.335 \times 10^{30}$  C m

dipole moment. In addition, low dipole moments for boron nanocages are due to the low charge of BN nanocage.

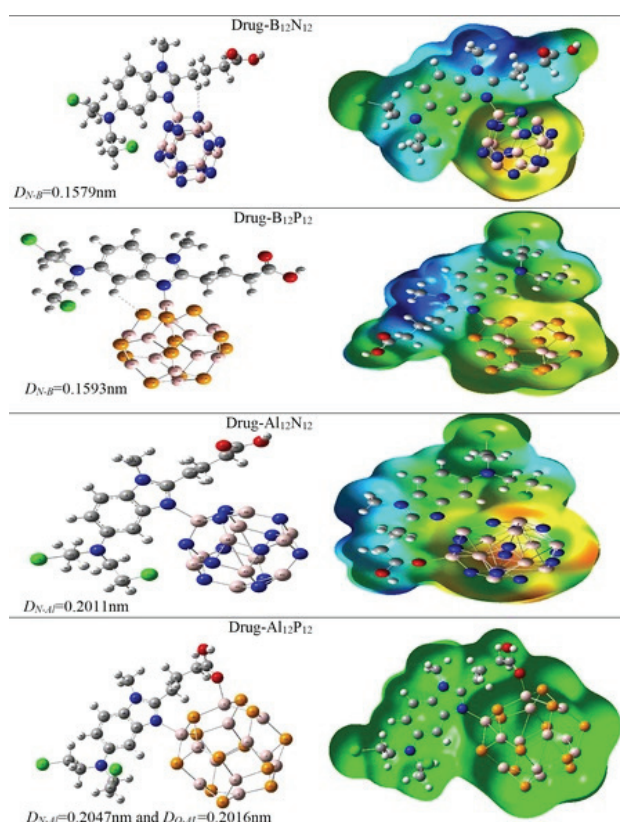


Fig. 3. Geometry optimizations and molecular electrostatic potential (MEP) maps of systems under study.

We investigated and assessed the active adsorption sites of the bendamustine drug-using Fukui function and MEPs analysis. The Gibbs energy changes ( $\Delta G$ ) according to Eq. (2), based on the most stable bendamustine nanocages in the gas and the solvent phases, are listed in Table III.

For all the other studied nanocages, large negative  $\Delta G$  values ( $\Delta G$  bendamustine- $B_{12}N_{12} = -70.50$  and  $-83.05$  kJ mol $^{-1}$ ,  $\Delta G$  bendamustine- $B_{12}P_{12} = -45.77$  and  $-48.78$  kJ mol $^{-1}$ ,  $\Delta G$  bendamustine- $Al_{12}N_{12} = -117.57$  and  $-126.18$  kJ mol $^{-1}$  and  $\Delta G$  bendamustine- $Al_{12}P_{12} = -98.95$  and  $-109.53$  kJ mol $^{-1}$ ) in the gas and solvent phases are obtained and could be represented as covalent interactions. These interactions are exothermic thermodynamically and have shown chemisorption adsorption. Therefore, studied nanocages adsorb bendamustine efficiently. Compared to the results of the adsorption of alprazolam drug

on the  $B_{12}N_{12}$  and  $Al_{12}N_{12}$  nanocages,<sup>37</sup>  $\Delta G$  value of  $Al_{12}N_{12}-B$  is similar to  $Al_{12}N_{12}-alprazolam$ , but  $\Delta G$  value of  $B_{12}N_{12}-B$  is less than  $B_{12}N_{12}-alprazolam$  and the complex formation process is spontaneous in all complexes.

The recovery time and sensibility of a sensor are essential parameters. The recovery time of a pharmaceutical molecule in drug delivery is fundamental characteristic in the drug adsorption. The desorption and release of the drug molecule are also momentous for a suitable sensor. Experimentally, the recovery process has been evaluated using UV light and high temperatures.<sup>38</sup>

Table III illustrates the recovery time for desorption of bendamustine drug from the surface of the studied nanocages in both the gas and the solvent phases. Recovery time is calculated from the transition state theory (TST):

$$\tau = \nu_0^{-1} \exp\left(\frac{-\Delta G_{ads}}{kT}\right) \quad (6)$$

where  $\nu_0$  is the frequency of attempt,  $k$  is the Boltzmann constant ( $8.3262 \text{ kJ mol}^{-1} \text{ K}^{-1}$ ) and  $T$  is temperature. An attempt frequency,  $\nu = 10^{12} \text{ s}^{-1}$ , has been applied to the recovery time for separating  $NO_2$  molecules from carbon nanotubes at room temperature.<sup>39</sup>

The trend of the recovery time, for desorption bendamustine drug from the surface of nanocages, are  $AlN > AlP > BN > BP$  in both phases which are in settlement with the trend of the Gibbs energy changes. Based on Eq. (6), more changes in Gibbs energy of adsorption causes a more extensive recovery time. According to obtained recovery times,  $Al_{12}N_{12}$  and  $Al_{12}P_{12}$  with a noticeable recovery time may not be a suitable sensor for bendamustine since bendamustine cannot desorb itself properly after adsorbing to  $Al_{12}N_{12}$  and  $Al_{12}P_{12}$  and could not be used as nano vehicle.

On the other hand, the recovery times for desorbing of bendamustine from BN and BP surfaces are low. These conclusions represented that the bendamustine drug can desorb from the  $B_{12}N_{12}$  and BP nanocages at a suitable time. As a result, the  $B_{12}N_{12}$  and BP nanocages can act as acceptable sensors for bendamustine.

In Fig. 4, DOS plots illustrated the number of states for both valence and conduction level of bendamustine were a little shifted with adsorbing on studied nanocages. Interaction bendamustine drug with nanocages is an electronically harmless interaction and would not change the properties of the drug. Because of their negative LUMO levels, the studied nanocages have a more considerable electron affinity also, due to a negative LUMO level, tend to capture electrons. In the formed complexes, the highest state occupied level, and the lowest state unoccupied level, the electronic contribution is related to the bendamustine drug, and no remarkable changes appeared.

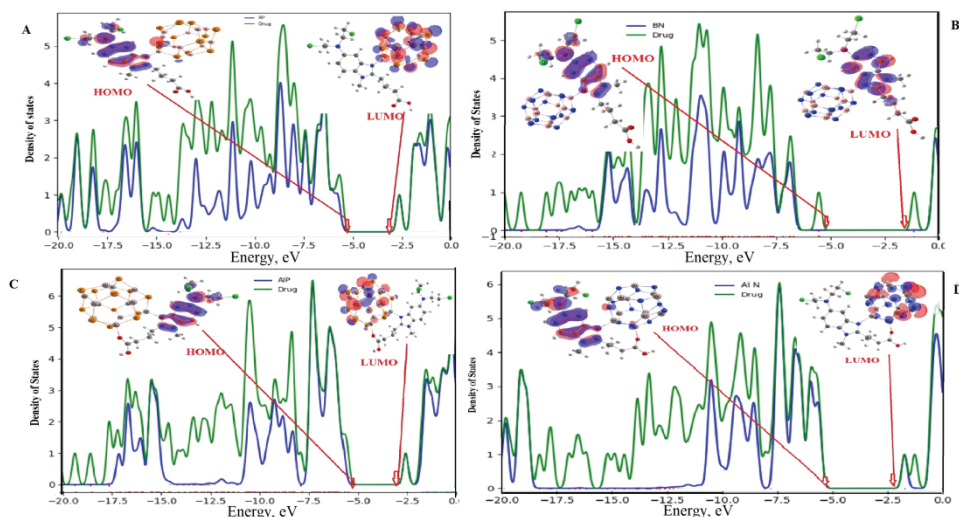


Fig. 4. Density of states for the complexation of:  $\text{B}_{12}\text{P}_{12}$  (A),  $\text{B}_{12}\text{N}_{12}$  (B),  $\text{Al}_{12}\text{P}_{12}$  (C) and  $\text{Al}_{12}\text{N}_{12}$  (D) with bendamustine drug at the B3LYP/6-31g (d,p) level of theory (PCM).

One of quantum chemistry methods for investigating the nature of bonds at interaction regions is the atoms in molecules (AIM) theory. This method uses concepts such as the Laplacian of the electron density,  $\nabla^2\rho(r)$  at the critical bond point (BCP), potential energy ( $V$ ), kinetic energy density ( $K$ ), electron density  $\rho(r)$  and, the total electronic energy density,  $H(r) = V(r) + K(r)$ , in terms of which the bond degree,  $H(r)/\rho(r)$ . As well, Eq. (6) represents a valuable relationship between them:<sup>40</sup>

$$\frac{1}{4}\nabla^2\rho(r) = V(r) + 2K(r) = H(r) + K(r) \quad (6)$$

If  $\nabla^2\rho(r) > 0$ , it displays electrostatic interactions, but in case  $\nabla^2\rho(r) < 0$  indicates the covalent bond.

Ionic interactions display positive Laplacian and  $H(r)$ ,  $\rho(r) < 0.1$ ,  $K(r)/\rho(r)$  and  $K(r)/V(r) > 1$ . The type of chemical bonds could be identified by the kinetic energy and potential energy values. The specifications of chemical bonds can be displayed by the values of the kinetic energy and potential energy. The type of chemical bonds is covalent if Laplacian and  $H(r)$  are negative,  $\rho(r) > 0.02$ ,  $K(r)/\rho(r)$  and  $K(r)/V(r) < 1$ . Parameters of AIM analysis at the bond critical points for the main chemical bonds of bendamustine drug nanocages are shown in Table IV.

$E(r)$  of bonds is negative in the gas and the water phases. Furthermore, the electron density values are higher than 0.02. The values of  $-K(r)/V(r)$ ,  $E(r)$  and  $\rho(r)$  descriptors indicated which of the formed bond between the bendamustine drug and studied nanocages are covalent.

TABLE IV. Topological parameters (all in atomic units) and ellipticity, at the B3LYP/6-31g (d,p) level of theory (PCM)

Complex	Bond	$\rho(r)$	$\nabla^2\rho(r)$	Ellipticity	$-K(r)/V(r)$	$K(r)/\rho(r)$	$E(r)$
$B_{12}N_{12}$	B3–N39	0.1384	0.2952	0.0504	0.6290	1.2998	-0.1061
$B_{12}P_{12}$	B12–N39	0.1384	0.3536	0.0430	0.6503	1.3808	-0.1028
$Al_{12}N_{12}$	N15–Al58	0.0453	0.3260	0.0386	0.9962	1.5839	-0.0002
$Al_{12}N_{12}$	O21–Al59	0.0453	0.3260	0.0386	1.1370	1.6040	0.0087
$Al_{12}P_{12}$	Al8–N39	0.0561	0.2898	0.0874	0.9783	1.3193	-0.0016
$Al_{12}P_{12}$	Al9–O45	0.0498	0.3218	0.0462	1.0735	1.5107	0.0051

## CONCLUSION

DFT calculations with the B3LYP/6–31G (d,p) method are used to study the interaction mechanism of the bendamustine drug with Al/B–N/P nanocages in both the gas and solvent phases. Relatively strong adsorptions occur between bendamustine and Al/B–N/P nanocages based on Gibbs energy changes. The negative values of the Gibbs energy change in all studied nanocages confirmed the spontaneous adsorption process. For bendamustine and Al/B–N/P nanocages complexes, the primary interaction mechanism is appropriate chemisorption. Optimized geometries and MEP indicate covalent interactions between the drug and nanocages. Despite, recovery time for desorption illustrated that the  $B_{12}N_{12}$  and  $B_{12}P_{12}$  nanovehicles for the bendamustine are more suitable than  $Al_{12}N_{12}$  and  $Al_{12}P_{12}$  nanocages. HOMO–LUMO and density of states diagrams indicate that nanocages slightly change the global charge distribution. The NBO analysis showed that the bendamustine drug's nitrogen atom is electron-donating, and the nanocages are the electron acceptor in all complexes. Also, the AIM results showed that the bond between studied nanocages and bendamustine is covalent. Nonetheless, all studied nanocages may be favorable candidates for detecting the bendamustine drug. However, we have deduced that pristine  $B_{12}P_{12}$  and  $B_{12}N_{12}$  nanocages are more suitable for drug delivery than  $Al_{12}P_{12}$  and  $Al_{12}N_{12}$ .

*Acknowledgement.* The authors are grateful to the Payame Noor University for encouragements.

## ИЗВОД

АДСОРПЦИЈА ЛЕКА ЗА РАК БИНДАМАСТИНА НА ЗАТВОРЕНИМ  
НАНОСТРУКТУРАМА Al/B–N/P: УПОРЕДНО DFT ПРОУЧАВАЊЕ

NOSRAT MADADI MAHANI, REZA BEHJATMANESH-ARDEKANI и ROYA YOSEFELAHI

*Department of Chemistry, Payame Noor University (PNU), 19395-4697, Tehran, Iran*

Третман лековима против рака путем затворених наноструктура (енгл. nanocages) је фармацеутски значајна због смањења споредних ефеката и отпуштања лека у близини туморске ћелије. Проучавали смо интеракцију лека против рака – биндамастина, са затвореним наноструктурама Al/B–N/P коришћењем теорије функционала густине (DFT) и у гасовитој и воденој фази на B3LYP/6-31G (d,p) нивоу теорије. Резултати

показују да се квантни параметри затворених наноструктура донекле мењају при адсорпцији лека биндамастина. Лек биндамастин делује као донор електрона и може да се адсорбује на електрон-акцепторском месту затворене наноструктуре. Промена Гибсове енергије одговара процесу хемисорпције у обе фазе. Резултати су показали да је веза између проучаваних затворених наноструктура и биндамастина ковалентна. Ипак, све проучаване затворене наноструктуре могу бити погодни кандидати за транспорт лека биндамастина. Међутим, на основу њихових времена опоравка закључујемо да су се чисте  $B_{12}P_{12}$  и  $B_{12}N_{12}$  затворене наноструктуре показале погоднијим за испоруку лека него  $Al_{12}P_{12}$  и  $Al_{12}N_{12}$ .

(Примљено 12. марта, ревидирано 25. маја, прихваћено 26. маја 2022)

#### REFERENCES

1. D. Nowak, S. Boehrer, A. Brieger, S. Z. Kim, S. Schaaf, D. Hoelzer, P. S Mitrou, E. Weidmann, K. U. Chow, *Leuk. Lymphoma* **45** (2004) 1429 (<https://doi.org/10.1080/1042819042000198858>)
2. J. W. Friedberg, P. Cohen, L. Chen, K. S. Robinson, A. Forero-Torres, A. S. La Casce, L. E. Fayad, A. Bessudo, E. S. Camacho, M. E. Williams, R. H. van der Jagt, J. W. Oliver, B. D. Cheson, *J. Clin. Oncol.* **26** (2008) 204 (<https://doi.org/10.1200/JCO.2007.12.5070>)
3. R. Kath, K. Blumenstengel, H. J. Fricke, K. Hoffken, J. *Cancer Res. Clin. Oncol.* **127** (2001) 48 (<https://doi.org/10.1007/s004320000180>)
4. Q. Weng, X. Wang, X. Wang, Y. Bando, D. Goldberg, *Chem. Soc. Rev.* **45** (2016) 3989 (<https://doi.org/10.1039/C5CS00869G>)
5. Q. Wang, Q. Sun, P. Jena, Y. Kawazoe, *ACS Nano* **3** (2009) 621 (<https://doi.org/10.1021/nn800815e>)
6. G. Ciofani, V. Raffa, A. J. Yu, Y. Chen, Y. Obata, S. Takeoka, A. Mencissi, A. Cuschieri, *Curr. Nanosci.* **5** (2009) 33 (<https://doi.org/10.2174/157341309787314557>)
7. P. A. Denis, F. Iribarne, *Comput. Theor. Chem.* **1164** (2019) 112538 (<https://doi.org/10.1016/j.comptc.2019.112538>)
8. P. A. Denis, S. Ullah, F. Iribarne, *New J. Chem.* **44** (2020) 5724 (<https://doi.org/10.1039/D0NJ00414F>)
9. P. A. Denis, *J. Phys. Org. Chem.* **25** (2012) 322 (<https://doi.org/10.1002/poc.1918>)
10. A. Soltani, A. Sousaraei, M. Bezi Javan, M. Eskandaric, H. Balakheyli, *New J. Chem.* **40** (2016) 7018 (<https://doi.org/10.1039/C6NJ00146G>)
11. C. A. Celaya, L. F. Hernandez-Ayala, F. B. Zamudio, J. A. Vargas, M. Reina, *J. Mol. Liq.* **329** (2021) 115528 (<https://doi.org/10.1016/j.molliq.2021.115528>)
12. N. Madadi Mahani, R. Yosefelahi, *Mor. J. Chem.* **6** (2018) 187 (<https://doi.org/10.48317/IMIST.PRSM/morjchem-v6i1.8619>)
13. J. S. Al-Otaibi, Y. Sheena Mary, Y. Shyma Mary, G. Serdaroglu, *J. Mol. Mod.* **27** (2021) 113 (<https://doi.org/10.1007/s00894-021-04742-z>)
14. K. A. Soliman, S. Abdel Aal, *Diam. Relat. Mater.* **117** (2021) 108458 (<https://doi.org/10.1016/j.diamond.2021.108458>)
15. A. Hosseiniyan, E. Vessally, A. Bekhradnia, K. Nejati, G. Rahimpour, *Thin Solid Films* **640** (2017) 93 (<http://dx.doi.org/10.1016/j.tsf.2017.08.049>)
16. V. de Paul Zoua, A. D. Tamafo Fouegue, D. B. Mama, J. N. Ghogomu, R. A. Ntieche, *Int. J. Quantum Chem.* **122** (2022) e26843 (<https://doi.org/10.1002/qua.26843>)

17. A. S. Rad, K. Ayub, *J. Alloys Compd.* **672** (2016) 161 (<https://doi.org/10.1016/j.jallcom.2016.02.139>)
18. Y. Zhao, N. E. Schultz, D. G. Truhlar, *J. Chem. Theory Comput.* **2** (2006) 364 (<https://doi.org/10.1021/ct0502763>)
19. *Gaussian 09*, Revision A.02, Gaussian, Inc., Wallingford, CT, 2016 (<https://gaussian.com/g09citation>)
20. N. Madadi Mahani, F. Sabermahani, A. Shamsolmaali, *Pak. J. Pharm. Sci.* **32** (6) (2019) 2741 (<https://doi.org/10.36721/PJPS.2019.32.6.REG.2741-2744.1>)
21. E. Vessally, S. Soleimani-Amiri, A. Hosseinian, L. Edjlali, A. Bekhradnia, *Physica, E* **87** (2017) 308 (<https://ui.adsabs.harvard.edu/abs/2017PhyE-87-308V>)
22. H. Xu, X. Tu, G. Fan, Q. Wang, X. Wang, X. Chu, *J. Mol. Liq.* **318** (2020) 114315 (<https://doi.org/10.1016/j.molliq.2020.114315>)
23. A. Hosseinian, E. Vessally, S. Yahyaei, L. Edjlali, A. Bekhradnia, *J. Clust. Sci.* **28** (2017) 2681 (<https://doi.org/10.1007/s10876-017-1253-6>)
24. B. Bankiewicz, P. Matczak, M. Palusiak, *J. Phys. Chem., A* **116** (2011) 452 (<https://doi.org/10.1021/jp210940b>)
25. A. Shokuh Rad, K. Ayub, *J. Alloys Comp.* **672** (2016) 161 (<https://doi.org/10.1016/j.jallcom.2016.02.139>)
26. M. Karan, V. Balachandran, M. Murugan, M. K. Murali, *Spectrochim. Acta* **130** (2014) 143 (<https://doi.org/10.1016/J.SAA.2014.03.128>)
27. V. V. Menon, E. Foto, Y. S. Mary, E. Karatas, C. Y. Panicker, G. Yalcin, S. Armakovic, S. J. Armakovic, C. V. Alsenoy, I. Yildiz, *J. Mol. Struct.* **1129** (2017) 86 (<https://doi.org/10.1016/J.MOLSTRUC.2016.09.059>)
28. Y. S. Mary, P. J. Jojo, C.Y. Panicker, C. Van Alsenoy, S. Ataei, I. Yildiz, *Spectrochim. Acta, A* **122** (2014) 499 (<https://doi.org/10.1016/J.SAA.2013.11.025>)
29. Y. S. Mary, P. J. Jojo, C. Y. Panicker, C. Van Alsenoy, S. Ataei, I. Yildiz, *Spectrochim. Acta, A* **125** (2014) 12 (<https://doi.org/10.1016/J.SAA.2014.01.068>)
30. P. Venkata Ramana, T. Sundius , S. Muthuc, K. Chandra Mouli, Y. Rama Krishna, K. Venkata Prasadd, R. Niranjana Devi, A. Irfanf, C. Santhamma, *J. Mol. Struct.* **1253** (2022) 132211 (<https://doi.org/10.1016/j.molstruc.2021.132211>)
31. Y. S. Mary, H.T. Varghese, C. Y. Panicker, M. Girisha, B. K. Sagar, H. S. Yathirajan, A. A. Al-Saadi, C. Van Alsenoy, *Spectrochim. Acta* **150** (2015) 543 (<https://doi.org/10.1016/j.saa.2015.05.090>)
32. B. R. Rajaraman, N. R. Sheela, S. Muthu, *Comput. Biol. Chem.* **82** (2019) 44 (<https://doi.org/10.1016/j.compbiochem.2019.05.011>)
33. R. Parr, W. Yang, *J. Am. Chem. Soc.* **106** (1984) 4049 (<https://doi.org/10.1021/ja00326a036>)
34. C. Martinez, M. Sedano, P. Lopez, *J. Mol. Graph. Model.* **28** (2009) 196 (<https://doi.org/10.1016/j.jmgm.2009.07.002>)
35. C. G. Zhan, J. A. Nichols,D. A. Dixon, *J. Phys. Chem., A* **107** (2003) 4184 (<https://doi.org/10.1021/jp0225774>)
36. A.Shokuh Rad, A. Ayub, *J. Alloys Cmpd.* **672** (2016) 161 (<https://doi.org/10.1016/j.jallcom.2016.02.139>)
37. S. Kaviani, S. Shahab, M. Sheikhi, *Phys. E: Low-Dimens. Syst. Nanostruct.* **126** (2021) 114473 (<https://doi.org/10.1016/j.physe.2020.114473>)

38. G. Seifert, P. W. Fowler, D. Mitchell, D. Porezag, Th. Frauenheim, *Chem. Phys. Lett.* **268** (1997) 352 ([https://doi.org/10.1016/S0009-2614\(97\)00214-5](https://doi.org/10.1016/S0009-2614(97)00214-5))
39. S. Peng, K. Cho, P. Qi, H. Dai, *Chem. Phys. Lett.* **387** (2004) 271 (<https://doi.org/10.1016/j.cplett.2004.02.026>)
40. P. Popelier, *J. Phys. Chem., A* **102** (1998) 1873 (<https://doi.org/10.1021/jp9805048>).